
Factors Predicting Metastatic Disease in ^{68}Ga -PSMA-11 PET-Positive Osseous Lesions in Prostate Cancer

Le Wen Chiu¹, Courtney Lawhn-Heath², Spencer C. Behr², Roxanna Juarez², Paola M. Perez¹, Iryna Lobach³, Matthew D. Bucknor², Thomas A. Hope², and Robert R. Flavell^{2,4}

¹*School of Medicine, University of California San Francisco, San Francisco, California;* ²*Department of Radiology and Biomedical Imaging, University of California San Francisco, San Francisco, California;* ³*Department of Epidemiology and Biostatistics, University of California San Francisco, San Francisco, California;* and ⁴*Department of Pharmaceutical Chemistry, University of California San Francisco, San Francisco, California*

Bone is the most common site of distant metastatic spread in prostate adenocarcinoma. Prostate-specific membrane antigen (PSMA) uptake has been described in both benign and malignant bone lesions, which can lead to false-positive findings on ^{68}Ga -PSMA-11 PET. The purpose of this study was to evaluate the diagnostic accuracy of ^{68}Ga -PSMA-11 PET for osseous prostate cancer metastases and improve bone uptake interpretation using semiquantitative metrics. **Methods:** Fifty-six prostate cancer patients (18 before prostatectomy and 38 with biochemical recurrence) who underwent ^{68}Ga -PSMA-11 PET/MRI or PET/CT examinations with osseous PSMA-ligand uptake were included in the study. Medical records were reviewed retrospectively by board-certified nuclear radiologists to determine true or false positivity based on a composite endpoint. For each avid osseous lesion, we measured biologic volume; size; PSMA Reporting and Data System (RADS) rating; SUV_{max} ; and ratio of lesion SUV_{max} to liver, blood pool, and background bone SUV_{max} . Differences between benign and malignant lesions were evaluated for statistical significance, and cutoffs for these parameters were determined to maximize diagnostic accuracy. **Results:** Among 56 participants, 13 (22.8%) had false-positive osseous ^{68}Ga -PSMA-11 findings and 43 (76.8%) had true-positive osseous ^{68}Ga -PSMA-11 findings. Twenty-two patients (39%) had 1 osseous lesion, 18 (32%) had 2–4 lesions, and 16 (29%) had 5 or more lesions. Cutoffs resulting in statistically significant ($P < 0.005$) differences between benign and malignant lesions were a PSMA RADS rating of at least 4, an SUV_{max} of at least 4.1, and SUV_{max} ratios of at least 2.11 for lesion to blood pool, at least 0.55 for lesion to liver, and at least 4.4 for lesion to bone. These measurements corresponded to a lesion-based ^{68}Ga -PSMA-11 PET lesion detection rate of 80%, 93%, 89%, 21%, and 89%, respectively, for malignancy, and a specificity of 73%, 73%, 73%, 93%, and 60%, respectively. **Conclusion:** PSMA RADS rating, SUV_{max} , and SUV_{max} ratio for lesion to blood pool can help differentiate benign from malignant lesions on ^{68}Ga -PSMA-11 PET. An SUV_{max} ratio of more than 2.2 for lesion to blood pool is a reasonable parameter to support image interpretation and presented a superior lesion detection rate and specificity when compared with visual interpretation by PSMA RADS. These parameters hold clinical value by improving diagnostic accuracy for metastatic prostate cancer on ^{68}Ga -PSMA-11 PET/MRI and PET/CT.

Key Words: PSMA PET; prostate cancer; osseous metastasis

J Nucl Med 2020; 61:1779–1785

DOI: 10.2967/jnumed.119.241174

Prostate cancer is the most common solid malignancy in men and the third leading cause of cancer-related mortality in the western world (1). There is strong emerging evidence to suggest that using PET probes that target prostate-specific membrane antigen (PSMA) can improve diagnostic accuracy and management in patients with prostate cancer (1–8). A variety of radiopharmaceuticals, including the ^{68}Ga -labeled PSMA inhibitor Glu-NH-CO-NH-Lys(Ahx)-HBED-CC, have been widely studied as imaging probes for PET and been shown to increase detection of prostate cancer in patients with biochemical recurrence (9,10) or with a new diagnosis of prostate cancer (11). Although only recently implemented into clinical practice, ^{68}Ga -PSMA PET demonstrated improved sensitivity and specificity compared with traditional imaging modalities such as bone scintigraphy, CT, and MRI in patients with primary intermediate- or high-risk disease (1,6,12).

Despite its name, however, PSMA is not solely prostate-specific. It also acts as a folate hydrolase that can be expressed in normal tissues and in both benign and malignant processes (13,14). For example, PSMA-ligand uptake can appear in conditions including but not limited to Paget disease, myelomas, fibrous dysplasia, hemangiomas, and bone fractures (15–20), which can represent false-positive findings for metastatic disease on ^{68}Ga -PSMA PET. Given the management implications of the presence of osseous metastatic disease and the potential for false-positives, guidelines have been suggested for interpreting ^{68}Ga -PSMA PET osseous lesions, including the PSMA Reporting and Data System (RADS) (21) and the Prostate Cancer Molecular Imaging Standardized Evaluation (22). Overall, recent studies suggest a high sensitivity and specificity for bone metastasis using ^{68}Ga -PSMA PET (20,23), superior to standard-of-care imaging including CT or bone scans. The purpose of this study was to evaluate the diagnostic accuracy of ^{68}Ga -PSMA-11 PET findings in the bone for prostate cancer metastasis and develop a framework for interpretation of these findings in patients with prostate adenocarcinoma.

MATERIALS AND METHODS

Subjects

This study was a secondary analysis of an institutional review board–approved prospectively acquired study of ^{68}Ga -PSMA-11 PET with two

Received Dec. 19, 2019; revision accepted Mar. 25, 2020.
For correspondence or reprints contact: Robert Flavell, University of California San Francisco, 505 Parnassus Ave., San Francisco, CA 94143.
E-mail: robert.flavell@ucsf.edu
Published online Apr. 17, 2020.
COPYRIGHT © 2020 by the Society of Nuclear Medicine and Molecular Imaging.

patient cohorts: one with a new diagnosis of prostate cancer and no definitive therapy, and a second with biochemical recurrence after definitive treatment (24,25). The study (NCT02611882, NCT02919111, NCT02918357, and NCT03353740) was performed under an investigational-new-drug application (IND 127621), with adjusted validation criteria. Overall, the records of 379 patients with a new diagnosis and 357 patients with biochemical recurrence were reviewed for the mention of abnormal osseous PSMA-ligand uptake in the imaging reports. This review yielded a cohort of 56 patients with a history of prostate cancer, including 18 with a new diagnosis and 38 with biochemical recurrence.

PET Image Acquisition and Reconstruction

An ITG germanium–gallium generator and an iQs fluidic labeling module (ITG) were used to prepare ^{68}Ga -PSMA-11 as previously described (26). An intravenous dose of 207.2 ± 55.5 MBq (range, 111–355.2 MBq) (5.6 ± 1.5 mCi; range, 3.0–9.6 mCi) of ^{68}Ga -PSMA-11 was administered. After an uptake period of 67 ± 14 min (range, 46–117 min), the patients underwent PET/CT (Discovery VCT; GE Healthcare) or PET/MRI (3.0-T time-of-flight Signa PET/MRI; GE Healthcare). For patients who underwent PET/CT, a 5-min acquisition per bed position was used from the pelvis through the mid abdomen, followed by 3-min acquisitions from the upper abdomen to the vertex. In the absence of a clinical contraindication, iodinated contrast medium (Omnipaque 350, 150 mL) was administered to all patients. A diagnostic CT scan was then obtained and used for both attenuation correction and morphologic evaluation (240 mA, 120 kV, 2-mm slice thickness). PET data were processed using iterative reconstruction with 4 iterations, 14 subsets, and a 168×168 matrix. The PET transaxial field of view was 620 mm. The axial PET slice thickness was 5.0 mm.

For patients who underwent PET/MRI, whole-body PET and whole-body T1- and T2-weighted coronal and axial MRI sequences were acquired simultaneously (3 min per bed position). Dedicated imaging of the abdomen and pelvis was also performed (8 min per bed position). In

the absence of clinical contraindications, gadolinium was administered, and a dynamic contrast-enhanced sequence was acquired through the pelvis followed by T2-weighted, diffusion-weighted, and postcontrast delayed T1-weighted imaging (26).

Composite Endpoint to Determine True- and False-Positive Bone Lesions

Bone lesions are not routinely biopsied to determine the presence of metastatic disease. Therefore, a composite endpoint to determine the presence or absence of metastatic disease was developed, as outlined on Figures 1 and 2. Two nuclear radiologists who had undergone 1 y of internship, 4 y of radiology residency, and 1 y of fellowship training in nuclear medicine and who were certified or board-eligible by the American Board of Nuclear Medicine, with 1.5 and 10 y of dedicated nuclear medicine experience, evaluated each focus of uptake above the background level in the bone as a true- or false-positive metastatic lesion. Cross-sectional imaging (CT or MRI) from the ^{68}Ga -PSMA-11 PET scan was available as an anatomic correlate. An experienced musculoskeletal radiologist with 8 y of dedicated experience was consulted to interpret equivocal findings. Differentiation of benign from malignant lesions was based on accepted criteria on anatomic CT or MRI (27).

^{68}Ga -Labeled PSMA PET Image Analysis

All images were reviewed in separate sessions by 2 other nuclear radiologists, with 1 and 9 y of dedicated nuclear medicine experience, who were unaware of the true- or false-positive determination above. Lesions were judged qualitatively by PSMA RADS and quantitatively by several SUV metrics, measured separately by both readers. Discrepancies in lesion determination were resolved by consensus.

Statistical Analysis

Sample characteristics were summarized by age, prior treatment, PSA level at the time of imaging, anatomic correlate, and Gleason score at diagnosis. Cutoffs for key parameters were inferred on the basis of the Youden index (28). Area under the receiver-operating-characteristic curve (AUC) and deLong 95% confidence interval (CI), which assesses the stability of the AUC estimate, were used to evaluate the ability of key parameters to determine diagnoses. Variable and location differences between benign and malignant lesions were calculated using the Student *t* test and the Fisher exact test. *P* values of less than 0.05 were considered statistically significant. Interrater reliability was evaluated with the Cohen κ -statistic, and strength of agreement was determined according to the definition described by Landis and Koch (29).

RESULTS

Patient Population

Of 736 patients who underwent ^{68}Ga -PSMA PET/CT or PET/MRI, 56 had abnormal PSMA-ligand uptake in the bones and qualified for this study (Fig. 1). The demographics of this study population are summarized in Table 1.

Determination of True and False Positivity by Composite Endpoint

A composite endpoint, outlined in Figure 2, was used to determine whether ^{68}Ga -PSMA PET findings were true-positive (i.e.,

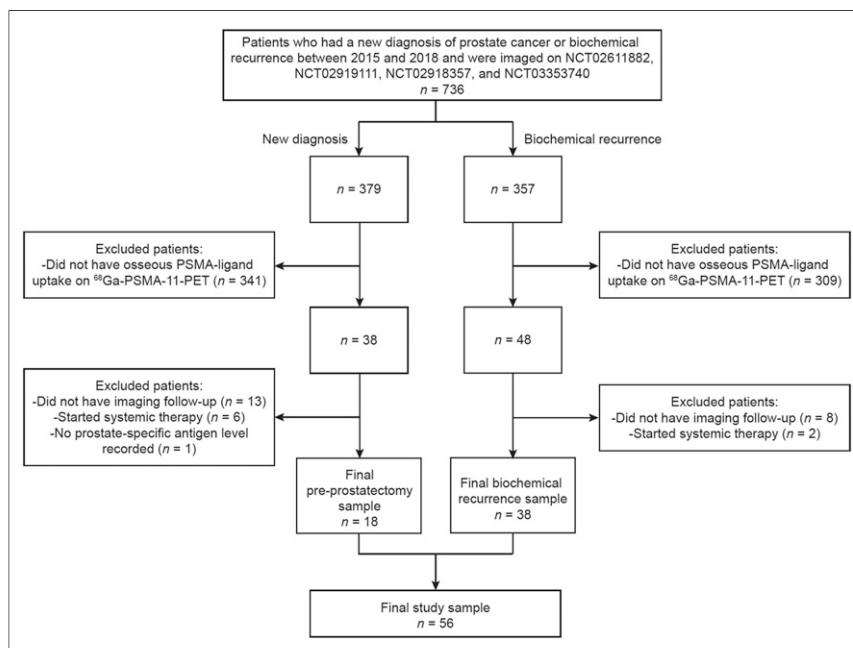


FIGURE 1. Flowchart showing inclusion and exclusion criteria by which preprostatectomy patients and patients who had biochemical recurrence of prostate cancer were selected for this study. Number of patients qualifying under each criterion is noted.

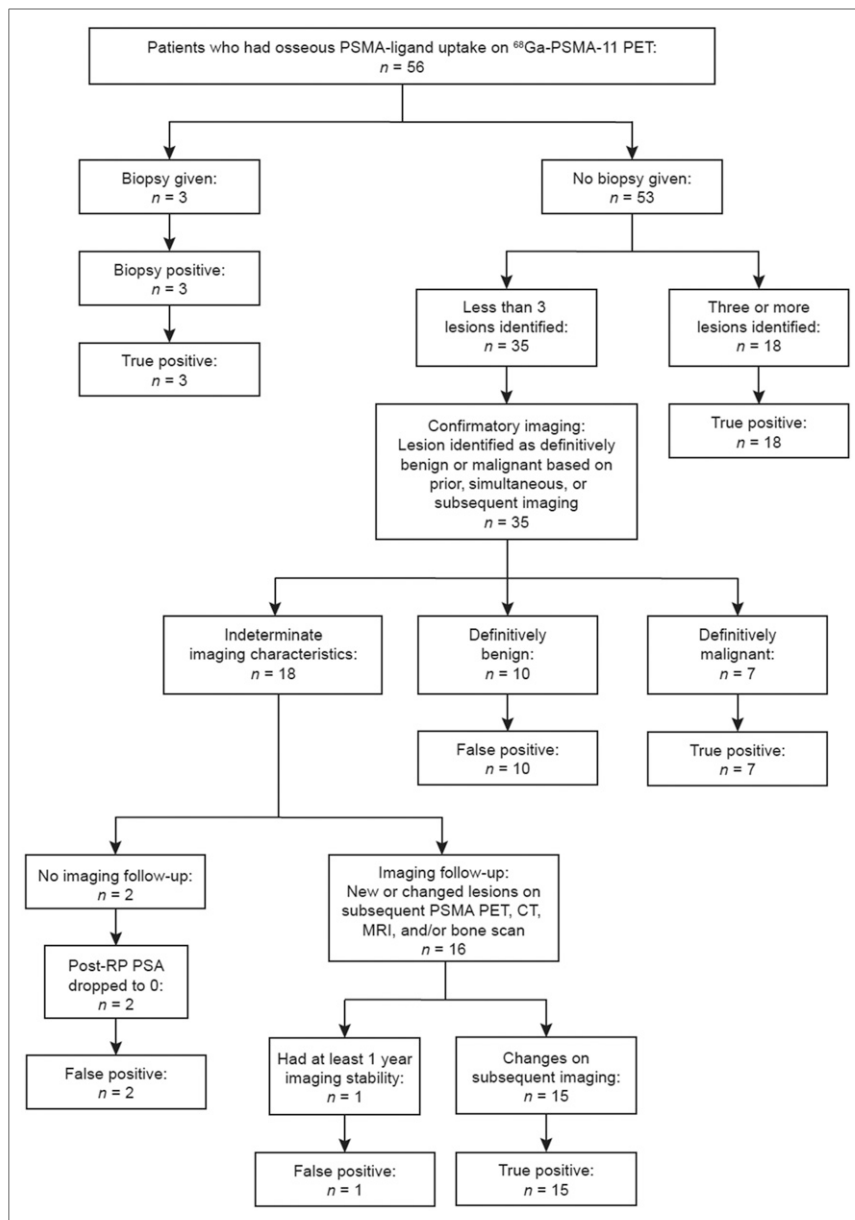


FIGURE 2. Flowchart showing process of patient-based lesion validation in this study of pre-prostatectomy patients and patients with biochemical recurrence of prostate cancer. Number of patients qualifying under each criterion is noted. In total, 43 patients had validated true-positive lesions and 13 had false-positive lesions. In case of multiple lesions with PSMA-ligand uptake, lesions were considered to be true-positive if 1 lesion was determined to be true-positive. True- and false-positive bone findings on imaging are aimed to be confirmed by biopsy if clinically feasible, by a multiplicity of lesions, by imaging follow-up, or by a drop in prostate-specific antigen level. RP = radical prostatectomy.

metastasis) or false-positive. Thirteen of 56 patients (23.2%) were determined to have false-positive lesions, and 43 of 56 patients (77.8%) were determined to have true-positive lesions. Forty true-positive lesions were determined by the multiplicity seen on PET/CT or PET/MRI or the confirmatory or follow-up imaging. One patient was considered to have a true-positive lesion due to changes on follow-up imaging and a PSA response after radiation to the metastasis (Fig. 3A). Three patients had pathologic correlation, wherein biopsy of the lesion revealed metastatic prostate cancer (Fig. 3B). Thirteen false-positive lesions were determined by confirmatory

imaging or imaging follow-up and subsequent stability on imaging for at least 1 y without definitive treatment. Two patients had their PSA drop to zero after prostatectomy and were considered as having false-positive lesions (Fig. 4). In contrast, 1 patient had a PSA that continued to rise after radiation therapy to a solitary lesion, which was considered false-positive (Supplemental Fig. 1; supplemental materials are available at <http://jnm.snmjournals.org>). Diagnoses for false-positive lesions are included in Table 2.

⁶⁸Ga-PSMA-11 PET Image Analysis, Detection Rate, and Uptake

Nineteen lesions were found in the ribs, 48 in the vertebrae, 30 in the pelvis, 12 in other appendicular regions, and 1 in the calvarium. There was no significant difference between the rate of true- and false-positive lesions by anatomic location (Supplemental Fig. 2). Among true-positive lesions, 15.8% (15/95) were found in the ribs, 42.1% (40/95) in the vertebrae, 29.5% (28/95) in the pelvis, 11.6% (11/95) in other appendicular locations, and 1% (1/95) in the calvarium. Among false-positive lesions, 26.7% (4/15) were found in the ribs, 53.3% (8/15) in the vertebrae, 13.3% (2/15) in the pelvis, 6.7% (1/15) in other appendicular locations, and 0% (0/15) in the calvarium.

Diagnostic accuracy by patient- and lesion-based analysis is shown in Table 3. Optimal cutoffs determined by receiver-operating-characteristic AUC analysis to differentiate metastases from benign lesions in a patient-based analysis were an SUV_{max} of at least 4.4 (95% CI, 0.70–0.99); an SUV_{max} ratio of at least 2.2 for lesion to blood pool (95% CI, 0.67–0.99), at least 1.33 for lesion to liver (95% CI, 0.62–0.99), and at least 7.11 for lesion to bone (95% CI, 0.74–0.98); a biologic volume of at least 0.62 cm^3 (95% CI, 0.35–0.71); a size of at least 1.8 cm (95% CI, 0.41–0.83); and a PSMA RADS rating of at least 4 (95% CI, 0.65–0.96). Optimal cutoffs in a lesion-based analysis were an SUV_{max} of at least 4.1 (95% CI, 0.69–0.96); an SUV_{max} ratio of at least 2.11 for lesion to blood pool (95% CI, 0.69–0.96), at least 0.55 for lesion to liver (95% CI, 0.62–0.91), and at least 4.4 for lesion to bone (95% CI, 0.71–0.94); a biologic volume of at least 0.52 cm^3 (95% CI, 0.36–0.68); a size of at least 1.8 cm (95% CI, 0.35–0.75); and a PSMA RADS rating of at least 4 (95% CI, 0.66–0.94). Receiver-operating-characteristic curves and AUC results are shown in Supplemental Figs. 3 and 4.

Patient- and lesion-based PSMA RADS ratings for total lesions had almost perfect interrater reliability (Table 4).

No statistical differences were found in mean size or biologic volume between benign and malignant lesions in either a patient-based or

TABLE 1
Clinical Characteristics of Study Sample

Characteristic	Value
Number of patients (n)	56
Mean age (y)	67.0 (range, 48–78; SD, ±7.9)
Prior treatment (n)*	
Radical prostatectomy	10 (13%)
Prostate bed radiation	9 (11%)
Metastasis-directed radiation	4 (5%)
Both radical prostatectomy and radiation therapy	14 (18%)
Androgen deprivation therapy or chemotherapy	28 (35%)
Other, unknown	9 (11%)
Currently undergoing androgen deprivation therapy or chemotherapy	6 (8%)
Median PSA level (ng/mL)	13.7 (range, 0.05–132.5)
PET/MR (n)	40 (71%)
PET/CT (n)	16 (29%)
Gleason score at diagnosis (n)	
3 + 3	5 (9%)
3 + 4	8 (14%)
4 + 3	8 (14%)
4 + 4	12 (21%)
4 + 5	13 (23%)
5 + 4	5 (9%)
5 + 5	2 (4%)
Not applicable	3 (5%)
PSMA PET findings (n)	
Bone lesions	
1 lesion	22 (39%)
2–4 lesions (oligometastatic)	18 (32%)
5+ lesions	16 (29%)
True-positive bone disease	43 (77%)
False-positive bone disease	13 (23%)
Lymph nodes	
None	26 (46%)
Pelvic only	13 (23%)
Nonregional only	6 (11%)
Pelvic and nonregional	11 (20%)
Other sites of metastatic disease	0 (0%)

*Prior treatment percentage applies only to patients with biochemical recurrence.

PSA = prostate-specific antigen.

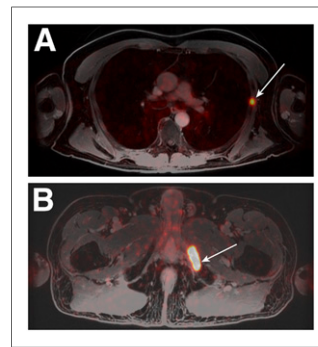


FIGURE 3. Examples of true-positive findings. (A) A 76-y-old man with biochemical recurrence of prostate cancer. Axial ⁶⁸Ga-PSMA-11 PET/MR image shows abnormal radiotracer uptake within left lateral sixth rib (arrow). PSA levels trended down after stereotactic body radiation therapy to rib. Lesion was considered true-positive. (B) A 66-y-old man with biochemical recurrence of prostate cancer. Axial ⁶⁸Ga-PSMA-11 PET/MR image shows abnormal radiotracer uptake within left pubic bone (arrow). Subsequent biopsy of left inferior pubic ramus revealed metastatic prostate cancer. Lesion was considered true-positive.

a lesion-based comparison (Supplemental Tables 1 and 2). In contrast, differences in the means of lesion SUV_{max}; SUV_{max} ratios to blood pool, liver, and bone; and PSMA RADS rating between benign and malignant lesions were statistically significant ($P < 0.005$) in both a patient-based and a lesion-based comparison.

DISCUSSION

This study was performed as a secondary analysis of patients who underwent ⁶⁸Ga-PSMA-11 PET/CT or PET/MR under a prospective research protocol. The goal of this study was to ascertain the diagnostic accuracy of this technique to detect osseous metastases. The substantial percentage of patients whose lesions were determined as true- or false-positive for metastatic disease based on confirmatory or follow-up imaging suggests that simultaneous CT or MRI is crucial for interpretation of ⁶⁸Ga-PSMA-11 PET.

Our study confirms the high diagnostic accuracy of SUV_{max} and PSMA RADS to distinguish between metastases and benign lesions that are PSMA-avid on ⁶⁸Ga-PSMA-11 PET/MRI and PET/CT. Among the parameters evaluated, SUV_{max} appears to be the most accurate and reliable PET parameter, with a statistically superior lesion detection rate, specificity, positive predictive value, and negative predictive value (Fig. 5). This conclusion is consistent with a prior analysis of bone lesions using DOTATOC PET in neuroendocrine tumors and in similar analyses of PSMA-ligand uptake in primary prostate lesions and in mediastinal lymph nodes (30,31). Moreover, since SUV_{max}

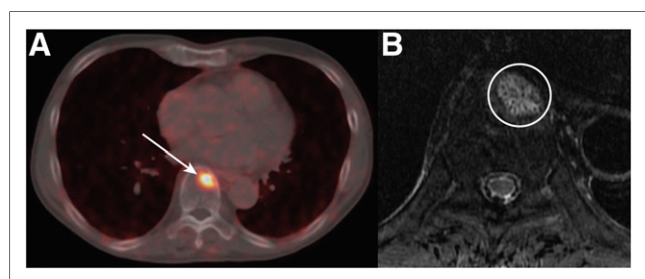


FIGURE 4. Example of false-positive findings. A 75-y-old man with prostate cancer, before prostatectomy, whose PSA dropped to 0 after prostatectomy. (A) Axial ⁶⁸Ga-labeled PSMA PET/CT image shows abnormal radiotracer uptake within T9 vertebral body (arrow). (B) Axial T2-weighted MR image through T9 vertebral body demonstrates high T2 signal lesion with trabeculated marrow appearance (circle). Findings suggest diagnosis of atypical hemangioma.

TABLE 2
Diagnoses of False-Positive Lesions

Diagnosis	Before prostatectomy	Biochemical recurrence
Hemangioma	2	1
Paget disease	1	0
Venous plexus	1	0
Degenerative	1	1
Indeterminate	5	4

Degenerative diagnosis includes degenerative disk disease and degenerative changes. Lesions for which no diagnosis was given were categorized as indeterminate.

is easily measured, it is a particularly useful parameter in characterizing lesions as malignant or benign in clinical practice.

A review of the independent factors and development of a combined model for analysis were not performed here. Therefore,

this study cannot conclude that SUV parameters are helpful for visually equivocal findings only. Our results complement the existing literature supporting the accuracy of ⁶⁸Ga-PSMA-11 PET to stage prostate cancer bone metastasis and its superiority to conventional imaging such as bone scans, CT, or MRI alone (20,32).

This study had several limitations. First, the study used patient data from a single center, introducing selection bias contingent on the particular patient population of this center. The lesion detection rate and specificity of ⁶⁸Ga-PSMA-11 PET/CT or MRI cannot be reasonably differentiated from the 736 patients to start with or the 56 to enter the study. Future studies should include larger cohorts, as the present study was limited by the small sample size and lack of prospective validation. Moreover, patients were identified for study inclusion via retrospective review of the radiology reports—a method that may cause some patients to be excluded because osseous lesions are missed on initial review. Second, this study used only a single radiopharmaceutical, ⁶⁸Ga-PSMA-11, whereas a multiplicity of tracers is currently under investigation. Prior studies have demonstrated different true- and false-positive findings based on the agents, with a notably higher false-positive rate for ¹⁸F-PSMA-1007 when compared with ⁶⁸Ga-PSMA-11 (30,33). Importantly, the presented findings are likely not relevant for ¹⁸F-ligands. Finally, cutoffs for the various measured parameters of ⁶⁸Ga-PSMA-11 uptake to differentiate

TABLE 3
Diagnostic Accuracy of PET Parameters to Detect Osseous Metastases

Characteristic	Cutoff	Sensitivity	Specificity	PPV	NPV
Patient-based analysis					
SUV _{max}	≥4.4	98% [0.87, 1.0] n = 54	62% [0.32, 0.86] n = 54	91% [0.78, 0.97] n = 54	90% [0.55, 1.0] n = 54
SUV_{max} ratio					
Lesion to blood pool	≥2.2	97% [0.87, 1.0] n = 53	69% [0.39, 0.91] n = 53	91% [0.78, 0.97] n = 53	90% [0.55, 1.0] n = 53
Lesion to liver	≥1.33	78% [0.62, 0.89] n = 53	77% [0.46, 0.95] n = 53	91% [0.76, 0.98] n = 53	53% [0.29, 0.76] n = 53
Lesion to bone	≥7.11	100% [0.91, 1.0] n = 53	31% [0.09, 0.61] n = 53	82% [0.68, 0.91] n = 53	100% [0.40, 1.0] n = 53
Biologic volume					
Size	≥1.8	50% [0.33, 0.67] n = 48	80% [0.44, 0.97] n = 48	90% [0.70, 0.99] n = 48	30% [0.14, 0.50] n = 48
PSMA RADS	≥4	93% [0.80, 0.98] n = 53	69% [0.39, 0.91] n = 53	90% [0.77, 0.97] n = 53	75% [0.43, 0.95] n = 53
Lesion-based analysis					
SUV _{max}	≥4.1	93% [0.86, 0.98] n = 107	73% [0.45, 0.92] n = 107	96% [0.89, 0.99] n = 107	65% [0.38, 0.86] n = 107
SUV_{max} ratio					
Lesion to blood pool	≥2.11	89% [0.80, 0.94] n = 104	73% [0.45, 0.92] n = 104	95% [0.88, 0.99] n = 104	52% [0.30, 0.74] n = 104
Lesion to liver	≥0.55	21% [0.13, 0.31] n = 104	93% [0.68, 1.0] n = 104	95% [0.75, 1.0] n = 104	17% [0.09, 0.26] n = 104
Lesion to bone	≥4.4	89% [0.80, 0.94] n = 104	60% [0.32, 0.84] n = 104	93% [0.85, 0.97] n = 104	47% [0.24, 0.71] n = 104
Biologic volume	≥0.52	89% [0.81, 0.95] n = 98	21% [0.05, 0.51] n = 98	87% [0.78, 0.93] n = 98	25% [0.05, 0.57] n = 98
Size	≥1.8	39% [0.28, 0.51] n = 85	80% [0.44, 0.97] n = 85	94% [0.79, 0.99] n = 85	15% [0.07, 0.27] n = 85
PSMA RADS	≥4	80% [0.70, 0.88] n = 104	73% [0.45, 0.92] n = 104	95% [0.87, 0.99] n = 104	38% [0.21, 0.58] n = 104

PPV = positive predictive value; NPV = negative predictive value.

Units for size are in centimeters, where clearly measurable lesion was present on anatomic imaging. SUV could not be accurately quantified in 2 cases because of technical error. Data in brackets are 95% CI.

TABLE 4
PSMA RADS Interrater Reliability

Group	K
Patient-based PSMA RADS rating for lesions with PSMA-ligand uptake	0.88
Lesion-based PSMA RADS rating for lesions with PSMA-ligand uptake	0.82

between true- and false-positive lesions for metastatic disease were determined by the Youden index.

CONCLUSION

Consideration of SUV_{max} , SUV_{max} ratio for lesion to blood pool, and PSMA RADS ratings for osseous lesions observed on ^{68}Ga -PSMA-11 PET enables high diagnostic accuracy for detecting prostate cancer osseous metastases. The current study demonstrated the importance of considering these parameters when interpreting equivocal findings on ^{68}Ga -PSMA-11 PET, along with the corresponding CT or MRI anatomic correlate. In particular, an SUV_{max} ratio of more than 2.2 for lesion to blood pool appears to be a reasonable parameter to support image interpretation, given the difficult reproducibility of ^{68}Ga SUV_{max} across different scanners. The SUV_{max} ratio for lesion to blood pool presented a superior lesion detection rate, specificity, positive predictive value, and negative predictive value when compared with visual interpretation by PSMA RADS. These findings establish criteria for radiologic interpretation of ^{68}Ga -PSMA PET to direct timely diagnosis and clinical management of patients with metastatic prostate cancer in the bone.

DISCLOSURE

This study was institutionally funded by the University of California San Francisco Summer Explore grant. Robert Flavell was also funded by a David Blitzer Prostate Cancer Foundation

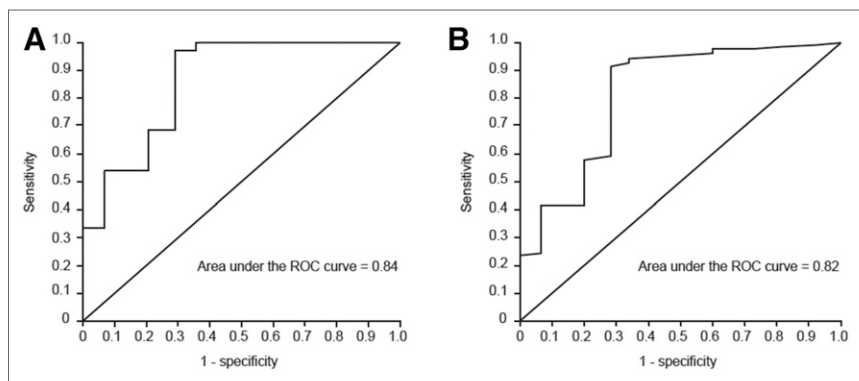


FIGURE 5. (A) Patient-based receiver-operating-characteristic curve for SUV_{max} of PSMA-avid osseous lesions ($n = 54$; 13 false-positive lesions and 41 true-positive lesions). AUC = 0.84; 95% CI = 0.70–0.99. (B) Lesion-based receiver-operating-characteristic curve for SUV_{max} of PSMA-avid osseous lesions ($n = 107$; 15 false-positive lesions and 92 true-positive lesions). AUC = 0.82; 95% CI = 0.69–0.96. ROC = receiver operating characteristic.

Young Investigator Award. No other potential conflict of interest relevant to this article was reported.

KEY POINTS

QUESTION: Which imaging findings are predictive of a true prostate cancer osseous metastasis?

PERTINENT FINDINGS: In this retrospective single-center study of 56 prostate cancer patients before prostatectomy or with biochemical recurrence who underwent ^{68}Ga -PSMA-11 PET/CT or PET/MRI, radiologic interpretation with consideration of SUV_{max} , PSMA RADS rating, and anatomic correlates was found to be essential for improving the diagnostic accuracy of ^{68}Ga -PSMA PET to detect prostate cancer metastasis to the bone. An SUV_{max} ratio of more than 2.2 for lesion to blood pool is a reasonable parameter to support image interpretation and presented a superior lesion detection rate, specificity, positive predictive value, and negative predictive value when compared with visual interpretation by PSMA RADS.

IMPLICATIONS FOR PATIENT CARE: Improved accuracy when interpreting ^{68}Ga -PSMA PET scans affects the timely and appropriate clinical management of patients with prostate cancer that has metastasized to the bone and can, furthermore, augment patient satisfaction and health-care savings by avoiding unnecessary treatment based on false-positive findings.

REFERENCES

- Hirmas N, Al-Ibraheem A, Herrmann K, et al. ^{68}Ga /PSMA PET/CT improves initial staging and management plan of patients with high-risk prostate cancer. *Mol Imaging Biol*. 2019;21:574–581.
- Uprimny C, Kroiss AS, Decristoforo C, et al. ^{68}Ga -PSMA-11 PET/CT in primary staging of prostate cancer: PSA and Gleason score predict the intensity of tracer accumulation in the primary tumour. *Eur J Nucl Med Mol Imaging*. 2017; 44:941–949.
- Zacho HD, Nielsen JB, Afshar-Oromieh A, et al. Prospective comparison of ^{68}Ga -PSMA PET/CT, ^{18}F -sodium fluoride PET/CT and diffusion weighted-MRI at for the detection of bone metastases in biochemically recurrent prostate cancer. *Eur J Nucl Med Mol Imaging*. 2018;45:1884–1897.
- Pyka T, Okamoto S, Dahlbender M, et al. Comparison of bone scintigraphy and ^{68}Ga -PSMA PET for skeletal staging in prostate cancer. *Eur J Nucl Med Mol Imaging*. 2016;43:2114–2121.
- Maurer T, Gschwend JE, Rauscher I, et al. Diagnostic efficacy of ^{68}Ga -PSMA positron emission tomography compared to conventional imaging for lymph node staging in 130 consecutive patients with intermediate to high risk prostate cancer. *J Urol*. 2016;195: 1436–1443.
- van Leeuwen PJ, Emmett L, Ho B, et al. Prospective evaluation of ^{68}Ga -PSMA-11 PET/CT for preoperative lymph node staging in prostate cancer. *BJU Int*. 2017;119:209–215.
- Fendler WP, Calais J, Eiber M, et al. Assessment of ^{68}Ga -PSMA-11 PET accuracy in localizing recurrent prostate cancer: a prospective single-arm clinical trial. *JAMA Oncol*. 2019;5:856–863.
- Sterzing F, Kratochwil C, Fiedler H, et al. ^{68}Ga -PSMA-11 PET/CT: a new technique with high potential for the radiotherapeutic management of prostate cancer patients. *Eur J Nucl Med Mol Imaging*. 2016;43: 34–41.
- Maurer T, Eiber M, Schwaiger M, Gschwend JE. Current use of PSMA-PET in prostate cancer management. *Nat Rev Urol*. 2016;13:226–235.
- Uprimny C, Kroiss AS, Fritz J, et al. Early PET imaging with ^{68}Ga -PSMA-11 increases the detection rate

- of local recurrence in prostate cancer patients with biochemical recurrence. *Eur J Nucl Med Mol Imaging*. 2017;44:1647–1655.
11. Budäus L, Leyh-Bannurah SR, Salomon G, et al. Initial experience of ⁶⁸Ga-PSMA PET/CT imaging in high-risk prostate cancer patients prior to radical prostatectomy. *Eur Urol*. 2016;69:393–396.
 12. Lengana T, Lawal IO, Boshomane TG, et al. ⁶⁸Ga-PSMA PET/CT replacing bone scan in the initial staging of skeletal metastasis in prostate cancer: a fait accompli? *Clin Genitourin Cancer*. 2018;16:392–401.
 13. Hofman MS, Hicks RJ, Maurer T, Eiber M. Prostate-specific membrane antigen PET: clinical utility in prostate cancer, normal patterns, pearls, and pitfalls. *Radiographics*. 2018;38:200–217.
 14. Pianou NK, Stavrou PZ, Vlontzou E, Rondogianni P, Exarhos DN, Datsaris IE. More advantages in detecting bone and soft tissue metastases from prostate cancer using ¹⁸F-PSMA PET/CT. *Hell J Nucl Med*. 2019;22:6–9.
 15. Artigas C, Alexiou J, Garcia C, et al. Paget bone disease demonstrated on ⁶⁸Ga-PSMA ligand PET/CT. *Eur J Nucl Med Mol Imaging*. 2016;43:195–196.
 16. Sasikumar A, Joy A, Pillai MR, Nanabala R, Thomas B. ⁶⁸Ga-PSMA PET/CT imaging in multiple myeloma. *Clin Nucl Med*. 2017;42:e126–e127.
 17. De Coster L, Sciot R, Everaerts W, et al. Fibrous dysplasia mimicking bone metastasis on ⁶⁸Ga-PSMA PET/MRI. *Eur J Nucl Med Mol Imaging*. 2017;44:1607–1608.
 18. Artigas C, Otte FX, Lemort M, van Velthoven R, Flamen P. Vertebral hemangioma mimicking bone metastasis in ⁶⁸Ga-PSMA ligand PET/CT. *Clin Nucl Med*. 2017;42:368–370.
 19. Jochumsen MR, Dias AH, Bouchelouche K. Benign traumatic rib fracture: a potential pitfall on ⁶⁸Ga-prostate-specific membrane antigen PET/CT for prostate cancer. *Clin Nucl Med*. 2018;43:38–40.
 20. Zacho HD, Nielsen JB, Haberkorn U, Stenholt L, Petersen LJ. ⁶⁸Ga-PSMA PET/CT for the detection of bone metastases in prostate cancer: a systematic review of the published literature. *Clin Physiol Funct Imaging*. 2017;38:911–922.
 21. Rowe SP, Pienta KJ, Pomper MG, Gorin MA. Proposal for a structured reporting system for prostate-specific membrane antigen–targeted PET imaging: PSMA-RADS version 1.0. *J Nucl Med*. 2018;59:479–485.
 22. Eiber M, Herrmann K, Calais J, et al. Prostate cancer molecular imaging standardized evaluation (PROMISE): proposed miTNM classification for the interpretation of PSMA-ligand PET/CT. *J Nucl Med*. 2018;59:469–478.
 23. Pomykala KL, Czernin J, Grogan TR, Armstrong WR, Williams J, Calais J. Total-body ⁶⁸Ga-PSMA-11 PET/CT for bone metastasis detection in prostate cancer patients: potential impact on bone scan guidelines. *J Nucl Med*. 2020;61:405–411.
 24. Hope TA, Aggarwal R, Chee B, et al. Impact of ⁶⁸Ga-PSMA-11 PET on management in patients with biochemically recurrent prostate cancer. *J Nucl Med*. 2017;58:1956–1961.
 25. Lawhn-Heath C, Flavell RR, Behr SC, et al. Single-center prospective evaluation of ⁶⁸Ga-PSMA-11 PET in biochemical recurrence of prostate cancer. *AJR*. 2019;213:266–274.
 26. Lake ST, Greene KL, Westphalen AC, et al. Optimal MRI sequences for ⁶⁸Ga-PSMA-11 PET/MRI in evaluation of biochemically recurrent prostate cancer. *EJNMMI Res*. 2017;7:77.
 27. Hakim DN, Pelly T, Kulendran M, Caris JA. Benign tumours of the bone: a review. *J Bone Oncol*. 2015;4:37–41.
 28. Habibzadeh F, Habibzadeh P, Yadollahie M. On determining the most appropriate test cut-off value: the case of tests with continuous results. *Biochem Med (Zagreb)*. 2016;26:297–307.
 29. Landis JR, Koch GG. The measurement of observer agreement for categorical data. *Biometrics*. 1977;33:159–174.
 30. Kuten J, Fahoum I, Savin Z, et al. Head-to-head comparison of ⁶⁸Ga-PSMA-11 with ¹⁸F-PSMA-1007 PET/CT in staging prostate cancer using histopathology and immunohistochemical analysis as a reference standard. *J Nucl Med*. 2020;61:527–532.
 31. Afshar-Oromieh A, Sattler LP, Steiger K, et al. Tracer uptake in mediastinal and paraaortal thoracic lymph nodes as a potential pitfall in image interpretation of PSMA ligand PET/CT. *Eur J Nucl Med Mol Imaging*. 2018;45:1179–1187.
 32. Sachpekidis C, Eder M, Kopka K, et al. ⁶⁸Ga-PSMA-11 dynamic PET/CT imaging in biochemical relapse of prostate cancer. *Eur J Nucl Med Mol Imaging*. 2016;43:1288–1299.
 33. Rauscher I, Krönke M, König M, et al. Matched-pair comparison of ⁶⁸Ga-PSMA-11 PET/CT and ¹⁸F-PSMA-1007 PET/CT: frequency of pitfalls and detection efficacy in biochemical recurrence after radical prostatectomy. *J Nucl Med*. 2020;61:51–57.